



Absolute radiant power measurement for the Au M lines of laser-plasma using a calibrated broadband soft X-ray spectrometer with flat-spectral response

Ph. Troussel, B. Villette, B. Emprin, G. Oudot, V. Tassin, F. Bridou, Franck Delmotte, M. Krumrey

► To cite this version:

Ph. Troussel, B. Villette, B. Emprin, G. Oudot, V. Tassin, et al.. Absolute radiant power measurement for the Au M lines of laser-plasma using a calibrated broadband soft X-ray spectrometer with flat-spectral response. *Review of Scientific Instruments*, 2014, 85 (1), pp.013503. 10.1063/1.4846915 . hal-01157538

HAL Id: hal-01157538

<https://hal.science/hal-01157538>

Submitted on 16 Nov 2015

HAL is a multi-disciplinary open access archive for the deposit and dissemination of scientific research documents, whether they are published or not. The documents may come from teaching and research institutions in France or abroad, or from public or private research centers.

L'archive ouverte pluridisciplinaire **HAL**, est destinée au dépôt et à la diffusion de documents scientifiques de niveau recherche, publiés ou non, émanant des établissements d'enseignement et de recherche français ou étrangers, des laboratoires publics ou privés.

Absolute radiant power measurement for the Au M lines of laser-plasma using a calibrated broadband soft X-ray spectrometer with flat-spectral response

Ph. Troussel,¹ B. Villette,¹ B. Emprin,^{1,2} G. Oudot,¹ V. Tassin,¹ F. Bridou,² F. Delmotte,² and M. Krumrey³

¹CEA/DAM/DIF, Bruyères le Châtel, 91297 Arpajon, France

²Laboratoire Charles Fabry, Institut d'Optique, CNRS, University Paris-Sud, 2, Avenue Augustin Fresnel, RD128, 91127 Palaiseau Cedex, France

³Physikalisch-Technische Bundesanstalt (PTB), Abbestr. 2-12, 10587 Berlin, Germany

(Received 17 June 2013; accepted 26 November 2013; published online 7 January 2014)

CEA implemented an absolutely calibrated broadband soft X-ray spectrometer called DMX on the Omega laser facility at the Laboratory for Laser Energetics (LLE) in 1999 to measure radiant power and spectral distribution of the radiation of the Au plasma. The DMX spectrometer is composed of 20 channels covering the spectral range from 50 eV to 20 keV. The channels for energies below 1.5 keV combine a mirror and a filter with a coaxial photo-emissive detector. For the channels above 5 keV the photoemissive detector is replaced by a conductive detector. The intermediate energy channels ($1.5 \text{ keV} < \text{photon energy} < 5 \text{ keV}$) use only a filter and a coaxial detector. A further improvement of DMX consists in flat-response X-ray channels for a precise absolute measurement of the photon flux in the photon energy range from 0.1 keV to 6 keV. Such channels are equipped with a filter, a Multilayer Mirror (MLM), and a coaxial detector. We present as an example the development of channel for the gold M emission lines in the photon energy range from 2 keV to 4 keV which has been successfully used on the OMEGA laser facility. The results of the radiant power measurements with the new MLM channel and with the usual channel composed of a thin titanium filter and a coaxial detector (without mirror) are compared. All elements of the channel have been calibrated in the laboratory of the Physikalisch-Technische Bundesanstalt, Germany's National Metrology Institute, at the synchrotron radiation facility BESSY II in Berlin using dedicated well established and validated methods. © 2014 AIP Publishing LLC. [<http://dx.doi.org/10.1063/1.4846915>]

I. INTRODUCTION

The absolute measurement of thermal X-ray flux emitted by a hohlraum in any laser experiment is an essential parameter which has to be precisely determined. In the experiments of indirectly driven inertial confinement fusion (ICF), the inner radiative hohlraum temperature T_r and its temporal behaviour are key parameters for designing and tuning indirectly driven implosions of a DT capsule. This temperature T_r can be inferred from the measured X-ray flux.

Numerous experiments^{1–5} have been performed to measure the X-ray flux on various laser interaction schemes in the range from 0.1 keV to 4 keV representing the main contribution to the X-ray emission.

In the indirect-drive scheme of inertial confinement fusion experiments, the capsule inserted in a high-Z hohlraum is compressed by the soft X-ray flux generated by the incident laser energy conversion on the hohlraum wall. The X-ray spectrum is composed of a thermal component with a radiation temperature up to 300 eV and a hard X-ray component. The spectrum part above 2 keV, especially gold M band radiation between 2 and 4 keV, is a source of capsule preheat which can preheat the capsule ablator with a low Z opacity as well as the capsule fuel. The X-ray flux is absorbed in the ablator, lowering the ablator density and causing an appreciable expansion of the inner shell. This preheat is creating an earlier shock than expected and a degraded

implosion performance with a low neutron emission. M-band radiation capsule preheat can be reduced by adding dopant in the ablator. M band fraction can be up to 15% of the totally hohlraum X-ray flux emitted. It is very important to know the temporal and spectral characteristics of the absolute X-ray flux. This accurately experimental characterization is essential to understand implosion experiments.

In the attempting ignition experiments with MJ class lasers such as National Ignition Facility (NIF)^{6,7} and Laser MégaJoule (LMJ),⁸ the temperature inside the hohlraum can be higher than $3 \times 10^6 \text{ K}$ (300 eV). Actually, the flux emitted from the “Laser Entrance Hole” (LEH) of the hohlraum is obtained by absolutely calibrated broadband X-ray spectrometers with a high temporal resolution of about 100 ps. The existing spectrometers Dante^{9,10} at LLNL and DMX¹¹ at CEA are based on transmitting bands in X-ray photon energy below a filter's K or L absorption edge. Both use photoemissive detectors with different photo-cathodes surface shapes (planar for Dante and cylindrical for DMX).

Figure 1 shows a scheme of a current typical mirror channel for energies used below 1.5 keV.

The grazing incidence mirror rejects the hard X-ray component transmitted through the filter, which consists of Mylar, Al Ti, Cu, etc., for the different channels. Moreover, the photocathode spectral sensitivity contributes to a better rejection because of the decreasing spectral responsivity with increasing photon energy.

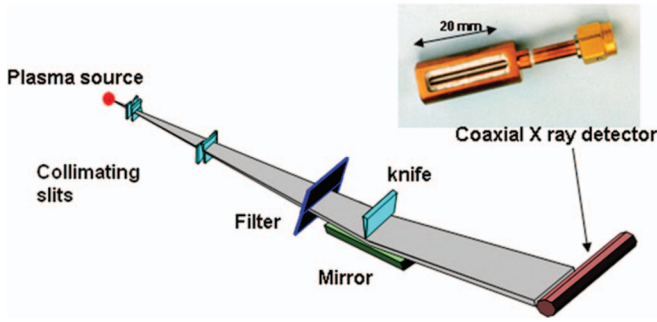


FIG. 1. DMX spectrometer setup showing one of the mirror channels.

The existing X-ray broadband channel for the range from 2 keV to 4 keV (Ti channel) consists of a $4\ \mu\text{m}$ Ti filter and a photoelectric coaxial detector. For the restitution of the measurements, we introduce in the simulation a theoretical M-band radiant power for which we adjust the amplitude. This contribution generates an uncertainty in the calculation which is important to eliminate. Therefore, we have developed additional novel flat-response X-ray channels consisting of a filter, a Multilayer Mirror (MLM), and a coaxial detector. The goal is time resolved absolute measurement of the photon flux in the energy range from 0.1 keV to 6 keV. We present here the channel for the photon energy range from 2 keV to 4 keV.

A team at the laboratory of Basic Plasma Physics in Hefei, China has proposed a very interesting novel flat-response X-ray detector and applied it on Shengguang laser facility.^{12,13} The detector consists of an X-ray diode and a compound filter. It shows the desired flatness of the spectral response inside the band but not outside the band. The absorption edges of the components limit the band and thus also the design options. Furthermore, there is no rejection of hard X-ray as there is no mirror included. Our idea to improve is using a MLM channel to greatly decrease the contribution to the measured response of the X-ray band.

The aim is to design a device with a spectral responsivity that is constant in the photon energy range from 2 keV to 4 keV and as low as possible outside this bandpass. The idea is to compensate the spectral response of the components (filter and detector) by the reflectance of a specifically designed mirror. A flat-response can be achieved by replacing the traditional mirror through a non-periodic MLM.

II. CONFIGURATION OF THE DMX SPECTROMETER FOR ABSOLUTE FLUX MEASUREMENT IN THE RANGE FROM 2 KEV TO 4 KEV

A. Standard configuration

The DMX spectrometer is used in routine at each shot with the existing broadband channel (Ti channel) for the range from 2 keV to 4 keV. It consists of a $4\ \mu\text{m}$ Ti filter and a photoelectric coaxial detector. Figure 2 shows the transmittance of the Ti filter, as well as the spectral responsivity of the aluminium photocathode coaxial detector and of the total channel. Obviously, the spectral responsivity varies within the channel. Therefore, a deconvolution method is required to obtain the spectral photon flux. More, the relative integrated

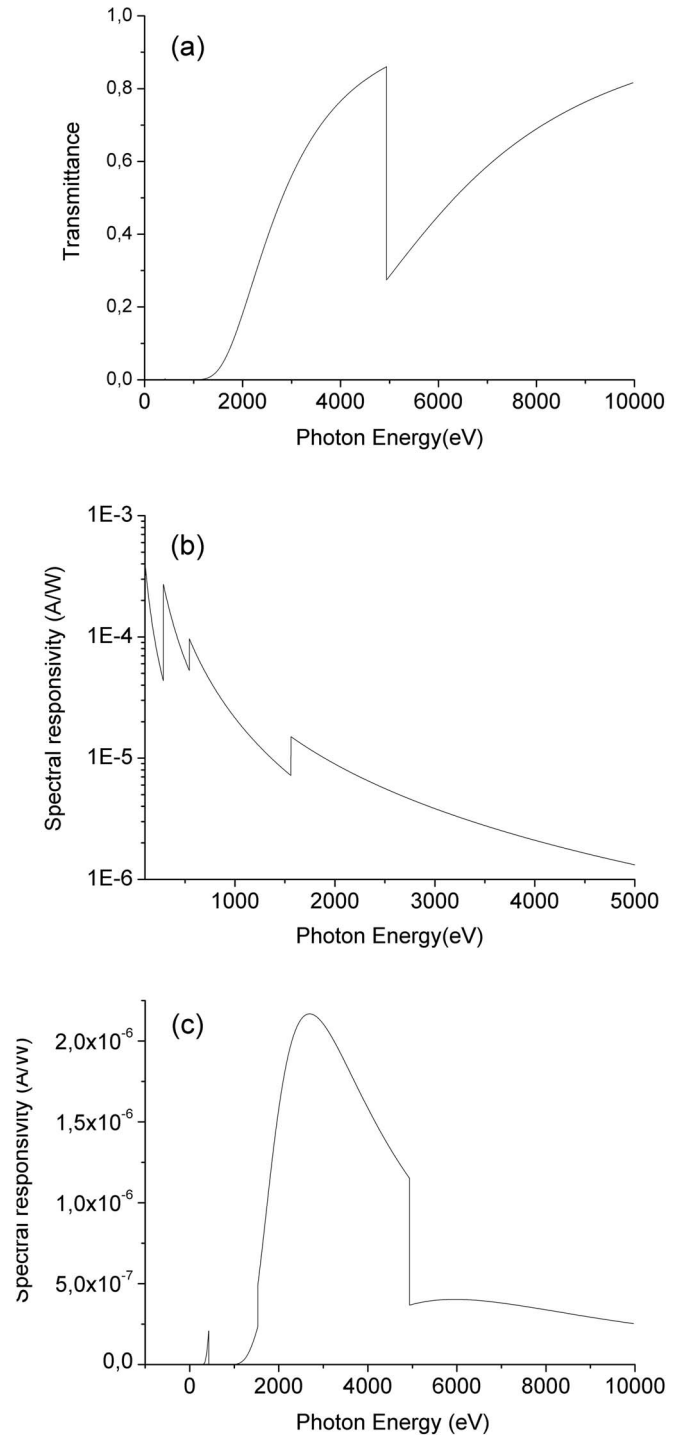


FIG. 2. Transmittance of the titanium filter (a); spectral responsivity of the aluminium photocathode coaxial detector (b), and the Ti channel total response in the current DMX (c).

spectral responsivity of this total channel inside the bandwidth is only 60%.

In the general case let us consider $s_{CH}(E) = \tau(E) \cdot \rho(E) \cdot s_{PK}(E)$, the total spectral responsivity of a channel at the photon energy E , where $\tau(E)$ is the filter transmittance, $\rho(E)$ is the mirror reflectance and $s_{PK}(E)$ is the spectral responsivity of the photocathode. In the case of the existing titanium channel, the total spectral responsivity is simplified to $s_{Ti}(E) = \tau(E) \cdot s_{PK}(E)$.

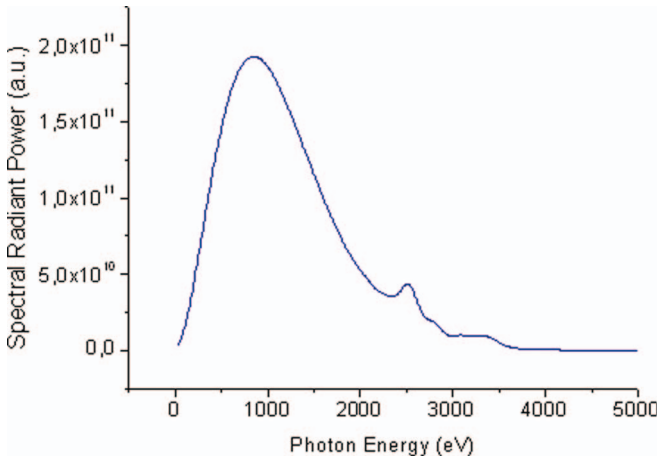


FIG. 3. Schematic spectral radiant power distribution of a gold laser plasma.

In a time-resolved measurement, the voltage $U_{Ti}(t)$ of the titanium channel generated by a spectral radiant power distribution $P(E, t)$ is given by

$$U_{Ti}(t) = R \cdot \Omega \cdot \int_0^\infty P(E, t) \cdot s_{Ti}(E) dE, \quad (1)$$

where R is the charge impedance (typically 50 Ohm) and Ω is the detection solid angle. If the responsivity varies with the energy in the channel, a deconvolution is required to obtain the radiant power from the measured voltage.

A schematic radiant power distribution of a gold laser plasma is shown in Fig. 3. It consists of a black-body spectrum with the spectral radiant power $P_p(E, t)$ that can be calculated from the temperature T_r according to Planck's law, and the superposed gold M-band radiation, which can be expressed as product of the theoretical M-band radiant power $P_{thMb}(E)$ and a time-dependent coefficient $k(t)$, leading to

$$U_{Ti}(t) = R \cdot \Omega \cdot \int_0^\infty [P_p(E, t) + k(t)P_{thMb}(E)]s_{Ti}(E) dE. \quad (2)$$

The coefficient $k(t)$ adjusts the amplitude of the absolute of the theoretical M-band radiant power so that the sum of both contributions reproduces exactly the signal level measured at each time. In this formalism, we consider that all the theoretical shape of the M-band radiant power $P_{thMb}(E)$ is constant or does not depend with time and disregard the fact that the intensity ratio between the gold M-emission lines can change with time.

The time-dependent hohlraum temperature $T_r(t)$, the total radiant power $P_{tot}(t)$, and the spectral radiant power $P_p(E, t)$ can be obtained from the measurements of the other DMX channels according to

$$P_{tot}(t) = \frac{\pi}{\cos \theta} \int_0^{E_{max}} P_p(E, t) dE = \sigma T_r^4(t) S, \quad (3)$$

where σ is the Stefan-Boltzmann constant, S is the emissive surface of the LEH, and θ is the observation angle with respect to the surface normal.

Taking into account that the coefficient $k(t)$ does not depend on the photon energy, and that the M-band radiant

power is mainly limited to the spectral range between 2 keV and 4 keV, Eq. (2) can be analyzed as

$$U_{Ti}(t) = R \cdot \Omega \int_0^\infty P_p(E, t) \cdot s_{Ti}(E) \cdot dE + R \cdot \Omega \cdot k(t) \times \int_{2 \text{ keV}}^{4 \text{ keV}} P_{thMb}(E) \cdot s_{Ti}(E) \cdot dE = U_p(t) + k(t) \cdot U_{thMb} \quad (4)$$

leading to

$$k(t) = \frac{U_{Ti}(t) - U_p(t)}{U_{thMb}} \quad (5)$$

$$\text{with } U_{thMb} = R \cdot \Omega \int_{2 \text{ keV}}^{4 \text{ keV}} P_{thMb}(E) \cdot s_{Ti}(E) \cdot dE \quad (6)$$

$$\text{and } U_p(t) = R \cdot \Omega \int_0^\infty P_p(E, t) \cdot s_{Ti}(E) \cdot dE. \quad (7)$$

B. MLM configuration

This measurement technique permits to restore directly the radiant power in the spectral window inside the range $\Delta E = E_{max} - E_{min}$ into the solid angle Ω from the measured signal. Therefore, a MLM channel can simplify this measurement and increase the accuracy. To measure the M-band X-ray from the 1 mm Au hohlraum, the mirror has been located at 3 m from the plasma, reducing the angular divergence to 0.03° . Because of its rectangular geometry (see Fig. 1), the coaxial detector is perfectly adapted to the beam after reflection on a mirror. Moreover, the mirror accepts the radiation from all the different areas in the X-ray. The X-ray emission of the plasma source is in fact not isotropic, but the DMX spectrometer measures not the total power but the radiant intensity (unit W/sr) which is compared to a calculation obtained in the same direction.

This flat-response channel has been first tested in December 2010 for hohlraum experiment on the OMEGA laser facility. Optimizing the hohlraum shape to reduce its surface area is a promising way to improve energetics of indirect drive targets.¹⁴

1. Design of the multilayer mirrors

The specifications of the channel require a wide bandpass and specific shape of the reflectance in the energy range from 2 keV to 4 keV. For energies below 2 keV and above 4 keV the reflectance has to be as low as possible, except the zone of the total reflection occurring on the top of the multilayer stack. To suppress the total reflection at energies below about 1.3 keV, a carbon-based filter like Mylar (CH) with a thickness of a few ten μm is required. For the MLM channel we can consider $s_{MLM}(E) = \tau_{CH}(E) \cdot \rho_{MLM}(E) \cdot s_{PK}(E)$, the total spectral responsivity of the channel at the photon energy E , where $\tau(E)$ is the CH filter transmittance, $\rho_{MLM}(E)$ is the

mirror reflectance, and $s_{PK}(E)$ is the spectral responsivity of the photocathode. Taking into account the spectral distribution of the radiation, we aimed for a factor 30 between the spectral responsivities inside and outside the desired energy range.

The use of non-periodic multilayer coating mirrors is necessary to enhance the bandwidth of the mirror reflectance. The concept of non-periodic multilayer was first proposed for neutrons optics under the name of super mirrors (1988), according to the Mezei model¹⁵ or Hayter¹⁶ and Mook model.¹⁷ Such structures consisted of a continuous variation of period in the multilayer from the substrate to the top in order to achieve a continuous variation of the Bragg wavelength and thus a widening of the spectral bandpass. Later, the non-periodic multilayer was developed for X-ray astrophysics and synchrotron radiation applications.^{18,19}

Up to now the design of non-periodic multilayer follows empirical laws inspired by the approaches used for visible light and neutron beams. Non-periodic multilayer design is a reverse optimization problem,²⁰ where the thicknesses of all layers composing the multilayer structure are considered as optimization independent parameters. The design and realization of the optical coating (in the development of broad bandwidth spectrometer) have been developed in close co-operation between CEA and the Laboratoire Charles Fabry in the Institut d'Optique (LCFIO). The thicknesses of the layers were designed and optimized with the help of a commercial code (TFCalc) with the needle procedure.²¹ This code, developed for visible domain, has been adapted for X-ray domain, by using appropriate data for the optical constants.²² In a second step the reflectance calculation is made precisely with the IMD code,²³ taking into account the low effect of the interfacial roughness (0.3 nm typically). The shape of the required mirror reflectance is calculated taking into account the transmittance of the CH ($C_{10}H_8O_4$) filter and of the spectral responsivity of the coaxial detector.

In most cases, solutions exist for the given shape of aimed reflectance. The grazing incidence angle of the mirror must be comprised between 1° and 2° due to the length of the mirror imposed by the mechanical design. For example, a grazing incidence angle of 1.5° leads to a mirror length of 77 mm for a 2 mm high entrance beam. Indeed, the reflectance decreases when this angle increases, but in order to have the possibility to filter the beam at low energies the zone where total reflection vanishes must be below 2 keV.

The choice of the materials and the determination of a theoretical formula of the multilayer by numerical simulation are detailed in Ref. 24. Among the available options, the material combination Cr/Sc provides good results and deposition parameters have been already optimized at the LCFIO to produce periodical multilayers.²⁵ The stack is protected from oxidation by a 3 nm thick top SiO_2 layer. Several designs have been realized to improve spectral shape and reflectance inside and outside the bandwidth.

As a first design, a stack of 101 layers and a SiO_2 top layer has been investigated (nomin1/MP10089). The calculated reflectance between 1 keV and 6 keV is compared to the desired shape in Fig. 4.

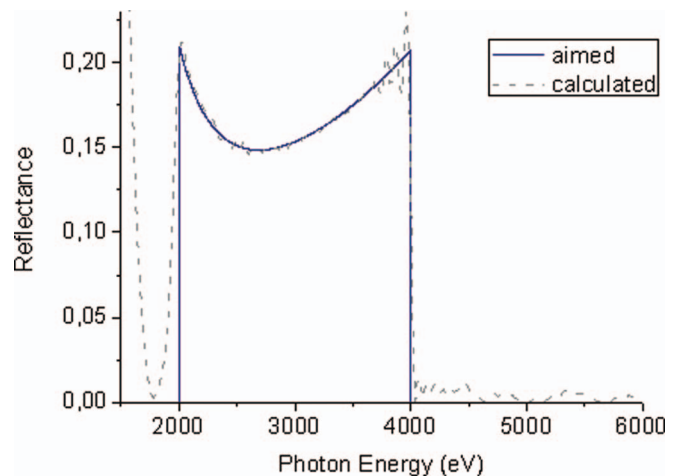


FIG. 4. Aimed mirror reflectance (thicker line) and calculated reflectance after optimization of various stacks; Sc/Cr ($N = 101$) + SiO_2 top layer.

This mirror (MP10089) has been used for the first experimental campaign. Suggested by the previous analysis, a new stack (90 layers), based on the previous 101 layers but without the first eleven ones has been made with a slightly improved reflectance (MP10095). The calculated thicknesses are comprised between 0.6 nm and 10 nm. For the second campaign, we have made a sample including a Si top single layer instead of a SiO_2 top layer (MP11085). The goal is to protect the Cr upper layer from the oxidation.²⁴ The Si layer is taken into account in the simulation.

2. Metrological characterization

The samples were prepared using magnetron sputtering in an apparatus described in Ref. 26. In order to characterize the multilayers also in terms of layer thicknesses, indices, and roughness, measurements have been performed at the synchrotron radiation facility BESSY II in the laboratory of the Physikalisch-Technische Bundesanstalt (PTB).²⁷

Scanning angle grazing-incidence X-ray reflectometry at fixed energies (2, 3, 4, and 8 keV) and also scanning energy X-ray reflectometry at 1.5° fixed incidence angle were conducted at the Four-Crystal Monochromator (FCM) beamline that covers the range from 1.75 keV to 10 keV in photon energy.²⁸ The mirrors were placed in a θ -2- θ reflectometer which provides 0.001° angular resolution for the sample and the detector. The typical beam size is 0.3 mm vertically \times 0.5 mm horizontally and the vertical beam divergence is about 0.02° . The geometric configuration of the synchrotron radiation calibration is very close to the configuration of the plasma experiment. The detector acceptance can be selected between 0.1° and 1° , the latter was used here. Silicon photodiodes with different apertures and a counting detector are mounted on the detector arm. The reflectance was determined as the ratio of the current for one of these diodes in the reflected beam to its current in the direct beam. To take into account the variations in the incident monochromatic photon flux, the currents are normalized to the current of a thin photodiode operating in transmission mode placed in front of the reflectometer.

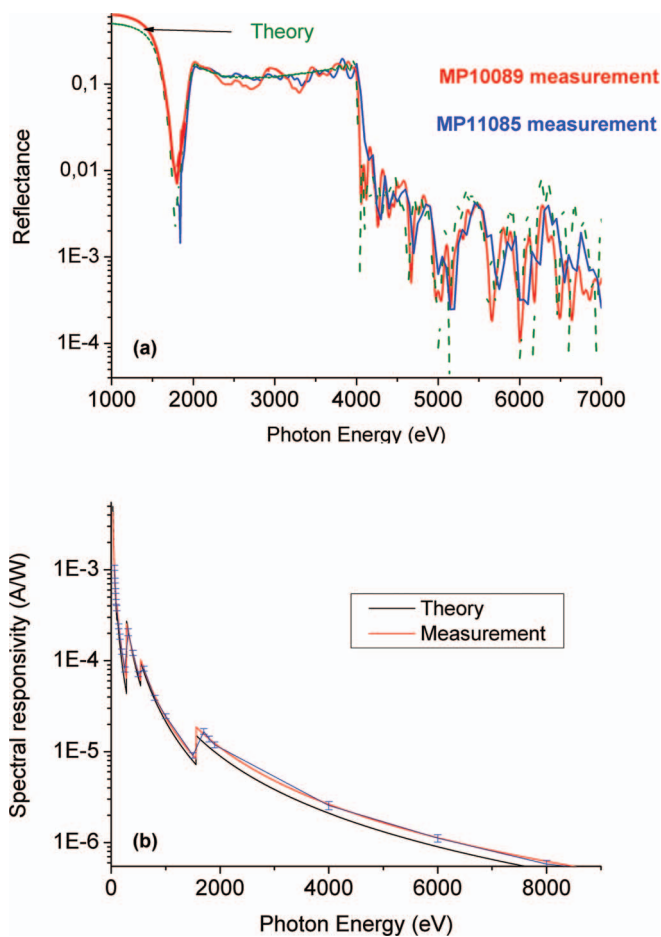


FIG. 5. Measured reflectance of two multilayer mirrors (MP10089 and MP11085) (a) and spectral responsivity of the coaxial photoemissive detector (b) compared to theoretical values.

A measured energy scan at 1.5° grazing angle is shown in Fig. 5(a) for both mirrors in comparison with the initially calculated reflectance.

The mirror homogeneity has been checked by moving its surface under the X-ray beam along the long axis. The measured reflectance comes close to the calculation and the spectral contrast of the filter bandwidth is high: we have only 3% of the maximum reflectance outside the 2 keV to 4 keV range, but some oscillations appear within the bandwidth. A possible source of these oscillations comes from interferences between the deeper thicknesses, because there is a small variation between the designed (or expected) and obtained thicknesses. We see an improvement for mirror MP11085 due to suppression of the first eleven layers and the silicon protective layer.

The spectral responsivity of the coaxial photoemissive detector has also been measured at the FCM beamline and at the SX700²⁹ beamline that covers the range from 0.05 keV to 1.9 keV, as shown on Fig. 5(b). At both beamlines, the calibration is based on calibrated photodiodes which in turn were calibrated against a cryogenic radiometer as a primary detector standard.³⁰

The filter transmittance has been measured using the nearly monochromatic fluorescence emission from different targets on a 25 kV X-ray tube at CEA DIF.³¹

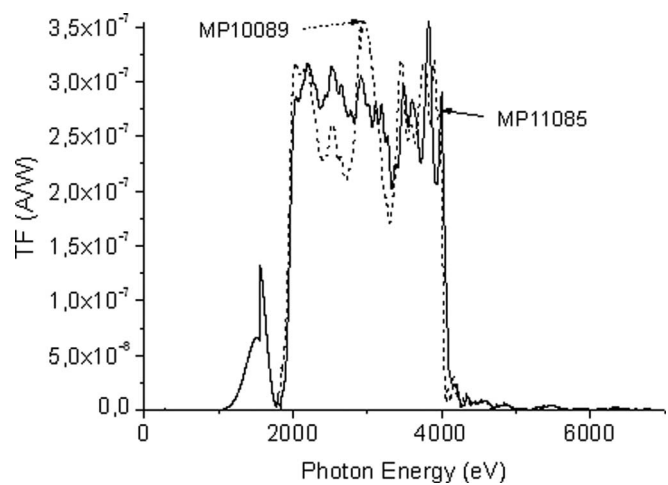


FIG. 6. Spectral responsivity of the MLM channel for two different mirrors.

The spectral responsivity of the MLM channel has been calculated from the measured spectral responses of the three components (filter, mirror, and detector). The results for both mirrors are shown in Fig. 6. In fact, the bandwidth with a high responsivity is from 1840 eV to 4260 eV. The relative integrated responsivity is 4.6% below 1840 eV and 0.3% above 4260 eV. The realization of the MLM channel is shown in Fig. 7. To take into account a typical gold laser plasma spectrum (neglecting its time dependence), we multiplied the responsivity with the spectrum shown in Fig. 3. For this product, the contributions outside the bandwidth are 20% below 1840 eV and 0.08% above 4260 eV. The realization of the MLM channel is shown in Fig. 7.

The relative uncertainty of the channel calibration is estimated to 15%. The CH filter is, like all the filters of the spectrometer, commercially available (Goodfellow Ltd.) and their thickness can be inhomogeneous over the surface of 5 mm \times 20 mm. Based on a density of 1.4 g/cm³, a thickness of 33 μ m has been obtained for the CH filter from transmission measurements. The uncertainty contributions from the CH filter transmission measurements are mainly the filter homogeneity over the working surface (1.3%), the current measurement (0.2%), and the beam stability (0.08%). The total expanded relative uncertainty is 2%, filters with larger inhomogeneities were rejected. Concerning the mirror, the

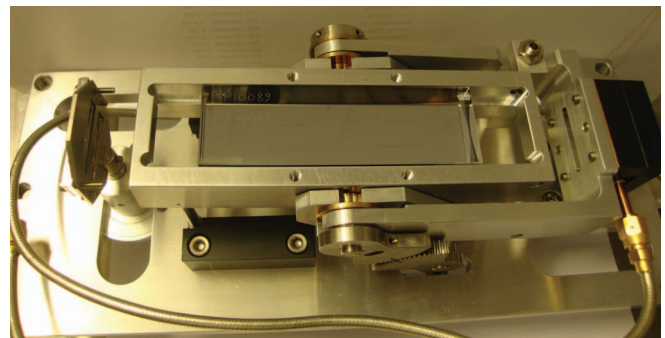


FIG. 7. Photo of the MLM channel with filter (left) and coaxial detector (right).

homogeneity has been checked by moving the surface under the X-ray beam along its dimension and relative uncertainty is estimated to be 1%. The estimated error on the grazing angle θ in the laser plasma measurements is 0.04° . We, therefore, measured the reflectance in the calibration measurements at PTB not only for the specified angle θ but also at $\theta \pm 0.04^\circ$ in order to estimate the influence on the reflectivity. An expanded relative uncertainty of 5% has been achieved for the reflectance. The expanded relative uncertainty of the spectral responsivity measurement of 8% for the photocathode coaxial detectors is dominated by the homogeneity (5%).

The total uncertainty for the radiant power determination is increased due to the remaining variations of the mirror reflectance.

III. EXPERIMENTAL RESULTS

This flat-response X-ray channel was tested on hohlraum experiments at the OMEGA laser facility of LLE.

In our experiment, the hohlraum is a millimeter size long gold-cylinder (or rugby) with two LEHs. About 40 frequency-tripled laser beams with 2.3 ns square temporal laser shape pulses irradiate the hohlraum wall from the two LEHs, delivering between 12 kJ and 17 kJ laser energy. The MLM channel measurement has been demonstrated with the one of Ti channel without mirror.

Figure 8 presents the result obtained on a shot. It shows the real agreement between the signal measured with the Ti channel and the signal calculated by the technique described before. Also shown is the signal calculated according to Planck's law without taking into account the M band radiation.

For the MLM channel, the mean responsivity s_{mean} in the range from 2 keV to 4 keV is 2.8×10^{-7} A/W as shown in Fig. 6. While the responsivity almost vanishes at energies above 4 keV, there is a remaining reflectance in the lower energy range between 1 keV and 1.8 keV. The signal U_{low} due

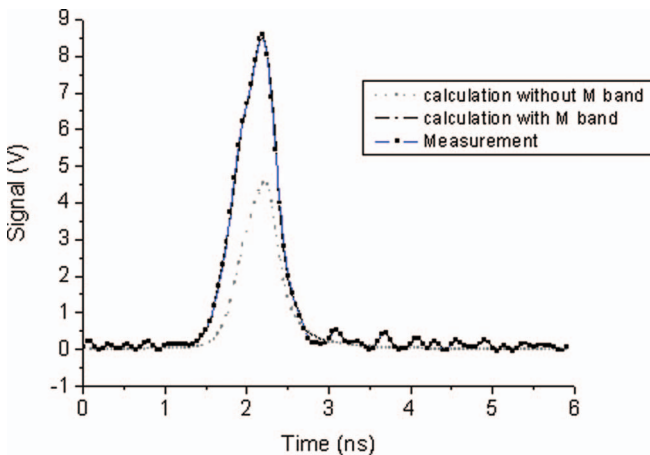


FIG. 8. Signal measured with the titanium channel and the signal calculated by the technique described before (cf. Sec. II). The grey curve was calculated with Planck's law without taking into account the gold M band radiation.

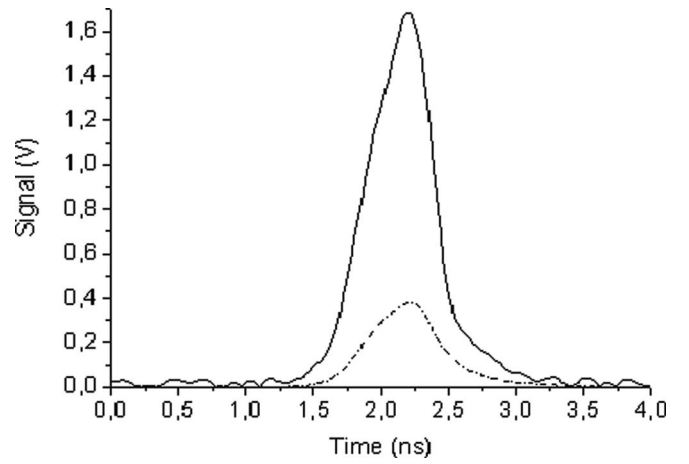


FIG. 9. Signal measured with the MP11085 MLM channel, designed for the spectral range from 2 keV to 4 keV, and signal part due to the remaining reflectance at lower photon energies (dashed).

to this contribution is

$$U_{\text{low}}(t) = R \cdot \Omega \int_{1000}^{1800} P_P(E, t) \cdot s_{\text{MLM}}(E) dE P. \quad (8)$$

The spectral radiant power $p(E, t)$ can be obtained from the measurements of four existing DMX channels covering that spectral range.¹¹

For this reason, the radiant power in the range between 2 keV and 4 keV is calculated using the corrected formalism of (7):

$$P_{\Delta E}(t) = \frac{U_{\text{MLM}}(t) - U_{\text{low}}(t)}{R \cdot \Omega s_{\text{mean}}}. \quad (9)$$

The measured signal and the contribution due to the reflectance at lower energies are shown in Fig. 9. The total emitted radiant power per solid angle in the range from 2 keV to 4 keV, obtained with the Ti channel and the new MLM channel, is shown in Fig. 10. We find a variation of 10% between these two channels. The MLM channel is more accurate for two reasons: better spectral contrast in the selected bandwidth and a calculation which does not take into account the

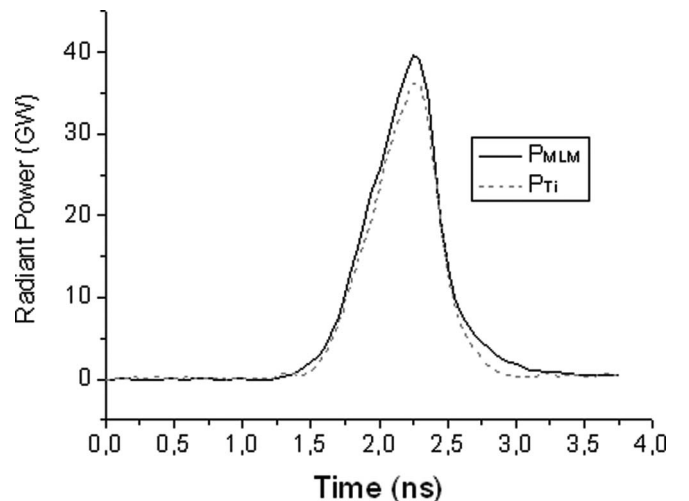


FIG. 10. The total emitted radiant power per solid angle in the range from 2 keV to 4 keV, obtained with the Ti channel and the new MLM channel.

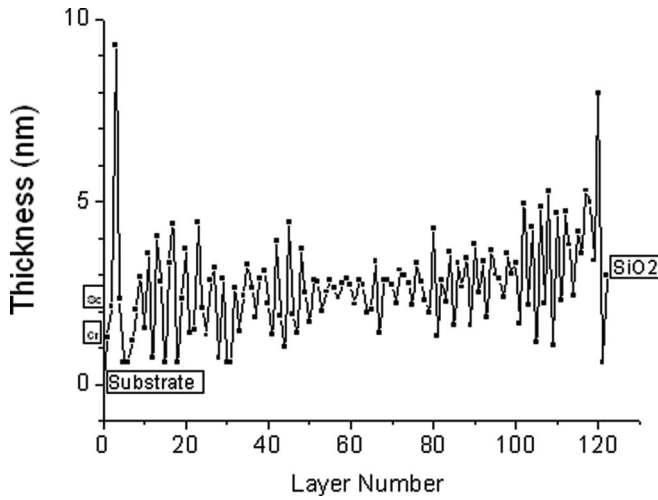


FIG. 11. Layer thicknesses for the optimized MLM designed for a grazing angle of 1.9° . The Cr layers are odd-numbered; the Sc layers are even-numbered.

2–4 keV Au M lines spectrum. With the MLM channel lower uncertainties will be obtained, especially if the remaining reflectance below 1.8 keV can be suppressed.

IV. FURTHER IMPROVEMENT OF THE MLM CHANNEL

To suppress the reflectance below 1.8 keV, the grazing incidence angle will be increased to 1.9° . Optimizations were done with the same commercial calculation code. The obtained new formula consists of 121 alternating Cr and Sc layers and a 3 nm thick SiO_2 top-layer. For good deposition homogeneity, the Cr and Sc layer thicknesses are comprised between 0.6 nm and 9.3 nm as shown in Fig. 11.

Taking into account the experimentally obtained optical constants, the diffusion between layers and an interface roughness in the range between 0.2 nm and 0.3 nm, the reflectance has been calculated and is displayed in Fig. 12. In order to suppress the total reflection, again a carbon-based filter with a thickness of $33 \mu\text{m}$ is used. The protective layer thickness is a key factor and has an important effect; small differences in thickness affect directly the reflectance (cf. Fig. 13). A tolerance of 0.6 nm at most is admissible, after that the reflectance characteristics are no longer fulfilled.

For the optimized channel consisting of a $33 \mu\text{m}$ thick Mylar filter, the optimized MLM at a grazing incidence angle of 1.9° , and a coaxial photoemissive detector, the calculated total responsivity comes very close to the desired constant value between 2 keV and 4 keV and vanishes outside this range as shown in Fig. 14.

If this MLM channel has an ideal constant spectral responsivity, the formalism can be simplified to

$$P_{\Delta E}(t) = \frac{U_{\text{MLM}}(t)}{R \cdot \Omega_{\text{MLM}}}. \quad (10)$$

The multiplication of the Au spectrum by the measured total responsivity gives now a relative area of only 3% below 1840 eV and 0.06% above 4260 eV.

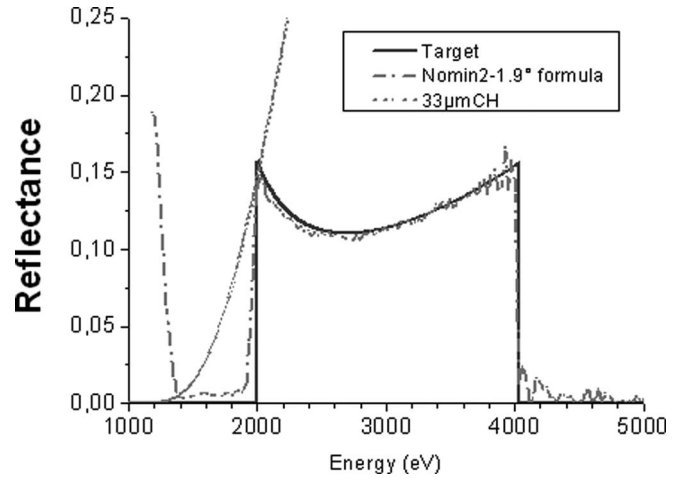


FIG. 12. Reflectance of the ideal mirror (solid line) and calculated reflectance according to the new formula (dashed-dotted line). Also shown is the transmittance of a carbon-based filter to suppress the surface reflectance below 1500 eV.

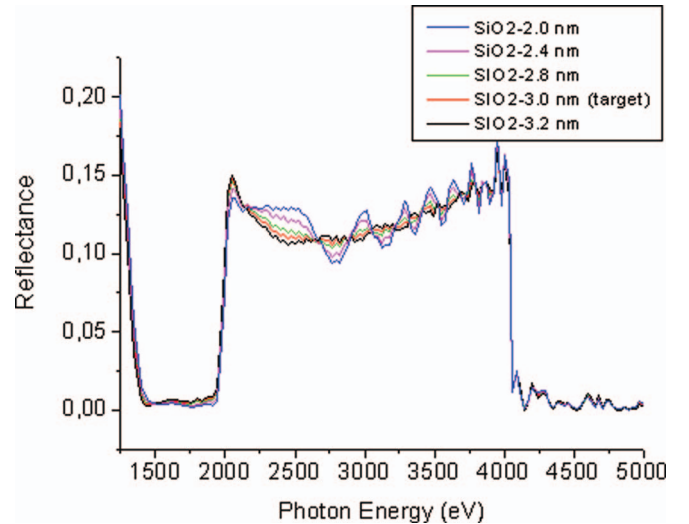


FIG. 13. Calculated reflectance of the mirror according to the new formula for different protective layer thicknesses.

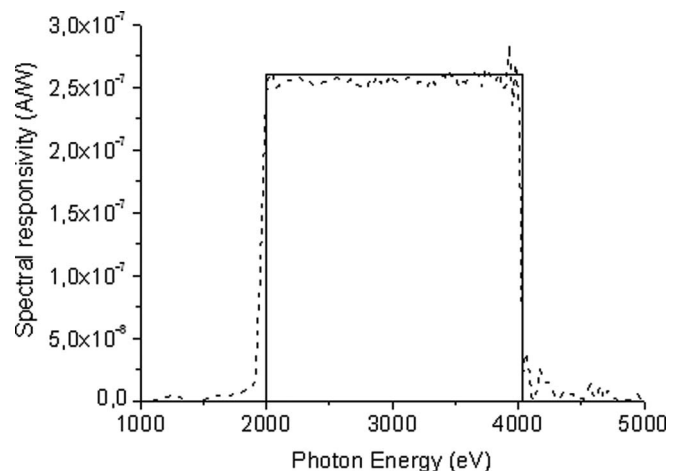


FIG. 14. Ideal spectral responsivity of the channel (solid line) and calculated total responsivity (dashed line).

V. CONCLUSION

We have developed and characterized a new flat-spectral response channel for the photon energy range from 2 keV to 4 keV, consisting of a 33 μm carbon-based filter, a photoemissive detector, and an optimized non-periodic multilayer mirror with alternating layers of Cr and Sc, operated at a grazing incidence angle of 1.5° . The channel is part of a broadband soft X-ray spectrometer which is used for laser plasma experiments and allows absolute radiant power measurements for the Au M lines. We have shown a further improvement of the MLM channel for the photon energy range from 2 keV to 4 keV suppressing the remaining reflectance below 1.8 keV by using a MLM working at a grazing incidence angle of 1.9° . We plan to develop a similar channel for the range from 4 keV to 6 keV using a 10 μm Fe filter and a different multilayer mirror with W and SiC layers, working at 1.3° grazing angle.

ACKNOWLEDGMENTS

All multilayer depositions have been carried out on the deposition machine at CEMOX (Centrale d'Elaboration et de Métrologie des Optiques X) implemented by PRAXO (Pôle d'Optique des Rayons X d'Orsay). The authors would like to thank C. Laubis, F. Scholze, S. Marggraf, and L. Cibik for measurements in the PTB laboratory at BESSY II in Berlin.

¹T. Boehly, *Rev. Sci. Instrum.* **66**, 508 (1995).

²D. Babonneau *et al.*, *Laser Part. Beams* **17**, 459 (1999).

³R. L. Kauffman *et al.*, *Phys. Rev. Lett.* **73**, 2320 (1994).

⁴D. R. Kania *et al.*, *Phys. Rev. A* **46**, 7853 (1992).

⁵D. Juraszek *et al.*, *J. Appl. Phys.* **70**, 1980 (1991).

⁶E. I. Moses, *Nucl. Fusion* **49**, 104022 (2009).

⁷D. Clery, *Science* **324**, 326 (2009).

⁸D. Besnard, *J. Phys. Conf. Ser.* **112**, 012004 (2008).

⁹H. G. Ahlstrom *et al.*, *J. Opt. Soc. Am.* **68**, 1731 (1978).

¹⁰C. Sorce, J. Schein *et al.*, *Rev. Sci. Instrum.* **77**, 10E518 (2006).

¹¹J. L. Bourgade, B. Villette, J. L. Bocher, J. Y. Boutin, S. Chiche, N. Dague, D. Gontier, J. P. Jadaud, B. Savale, and R. Wrobel, *Rev. Sci. Instrum.* **72**, 1173 (2001).

¹²Z. Li, X. Jiang *et al.*, *Rev. Sci. Instrum.* **81**, 073504 (2010).

¹³L. Guo, S. Li, J. Zheng, Z. Li, D. Yang, H. Du, L. Hou *et al.*, *Meas. Sci. Technol.* **23**, 065902 (2012).

¹⁴E. Vandenboomgaerde *et al.*, *Phys. Rev. Lett.* **99**, 065004 (2007).

¹⁵F. Mezei and P. A. Dagleish, *Commun. Phys.* **2**, 41 (1977).

¹⁶J. B. Hayter and H. A. Mook, *J. Appl. Crystallogr.* **22**, 35 (1989).

¹⁷Proc. SPIE **983**, Special issue: Thin-Film Neutron Optical Devices: Mirrors, Super mirrors, Multilayer Monochromators, Polarizers, and Beam Guides (1989).

¹⁸A. Erko, F. Schafers, B. Vidal-B, A. Yakshin, U. Pietsch, and W. Mahler, *Rev. Sci. Instrum.* **66**, 4845 (1995).

¹⁹P. Hoghoj, E. Ziegler, J. Susini, A. K. Freund, K. D. Joensen, P. Gorenstein, and J. L. Wood, *Nucl. Instrum. Methods Phys. Res. B* **132**, 528 (1997).

²⁰I. V. Kozhevnikov, I. N. Bukreeva, and E. Ziegler, *Nucl. Instrum. Methods Phys. Res. A* **460**, 424 (2001).

²¹TFCalc, Thin Film Design Software for Windows, Software Spectra, Inc., 14025 N. W. Hardvest Lane, Portland, OR 97229, USA, see www.spectra.com/support.

²²B. L. Henke, E. M. Gullikson, and J. C. Davis, *At. Data Nucl. Data Tables* **54**, 181 (1993).

²³D. Windt, *Comput. Phys.* **12**, 360 (1998).

²⁴F. Bridou, F. Delmotte, Ph. Troussel, and B. Villette, *Nucl. Instrum. Methods Phys. Res. A* **680**, 69 (2012).

²⁵A. Hardouin, Thesis, Université Paris-Sud, Orsay, France, 2007; <http://tel.archives-ouvertes.fr/tel-00265515/avet>.

²⁶J. Gautier, F. Delmotte, M. Roulliay, F. Bridou, M.-F. Ravet, and A. Jérôme, *Appl. Opt.* **44**, 384 (2005).

²⁷B. Beckhoff, A. Gottwald, R. Klein, M. Krumrey, R. Müller, M. Richter, F. Scholze, R. Thornagel, and G. Ulm, *Phys. Status Solidi B* **246**, 1415 (2009).

²⁸M. Krumrey and G. Ulm, *Nucl. Instrum. Methods Phys. Res. A* **467–468**, 1175 (2001).

²⁹R. Klein, C. Laubis, R. Müller, F. Scholze, and G. Ulm, *Microelectron. Eng.* **83**, 707 (2006).

³⁰A. Gottwald, U. Kroth, M. Krumrey, M. Richter, F. Scholze, and G. Ulm, *Metrologia* **43**, S125 (2006).

³¹L. Beck, P. Stemmler, G. Ban, B. Villette, V. Frotté, C. Bizeuil, J. Y. Boutin, and C. Nazet, *Nucl. Instrum. Methods Phys. Res. A* **369**, 401 (1996).

Review of Scientific Instruments is copyrighted by the American Institute of Physics (AIP). Redistribution of journal material is subject to the AIP online journal license and/or AIP copyright. For more information, see <http://ojps.aip.org/rsio/rsicr.jsp>